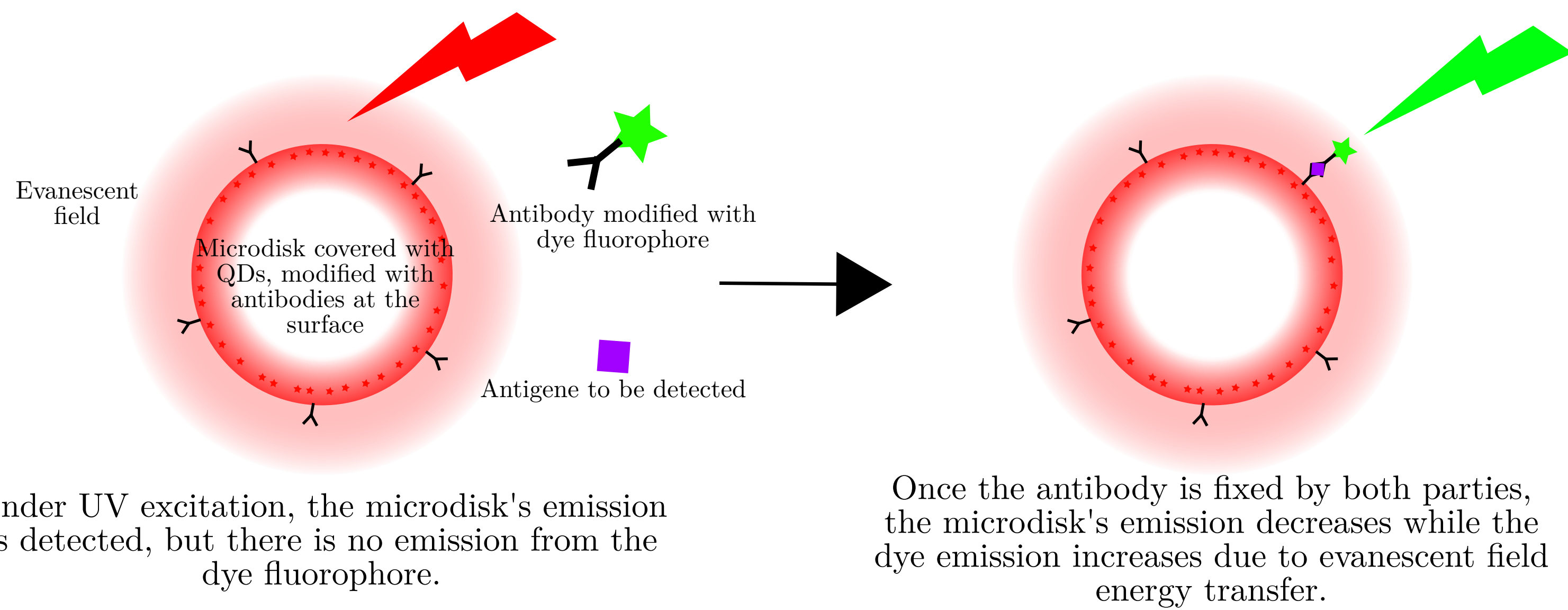
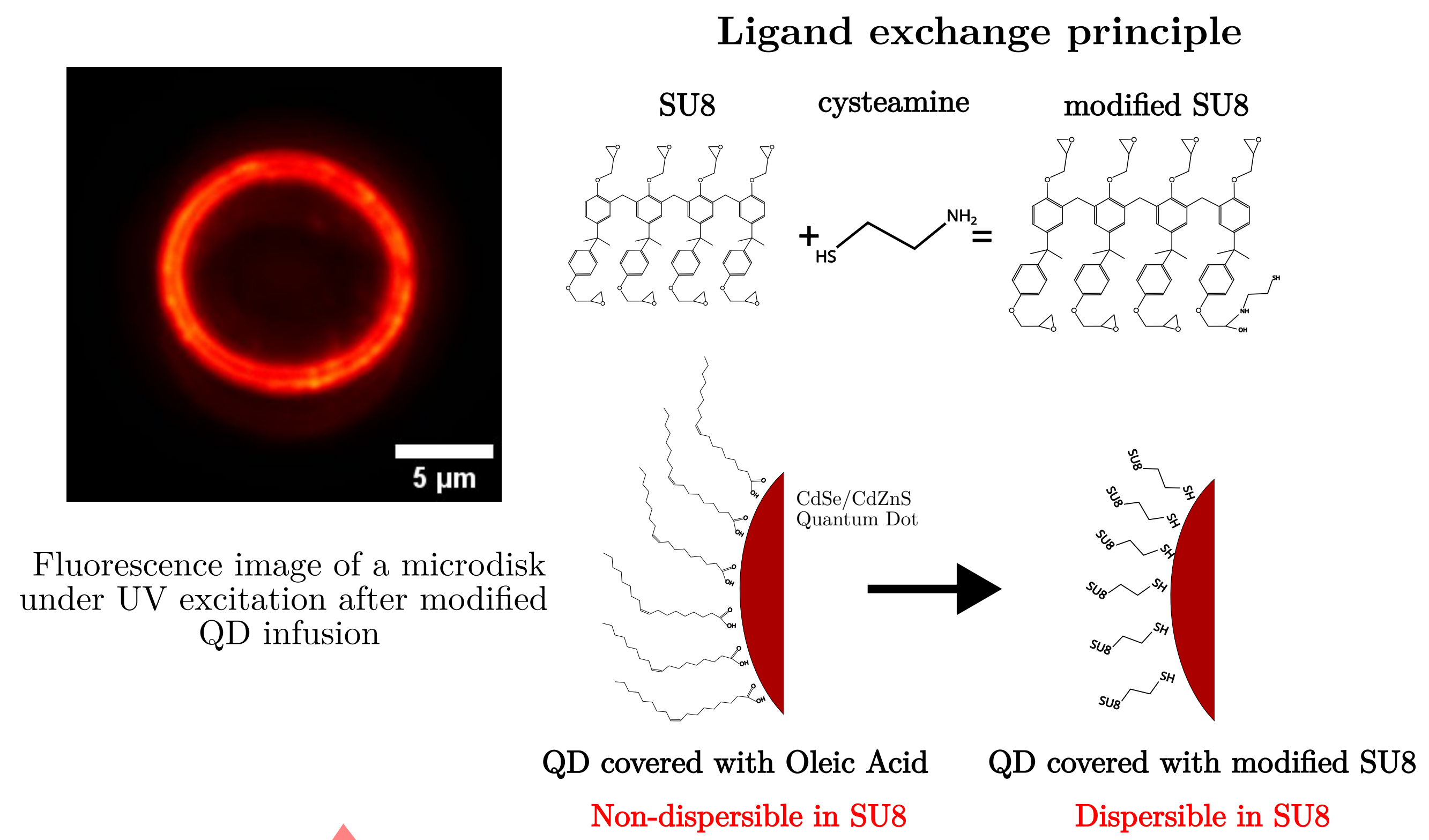


## Towards Biological Detection



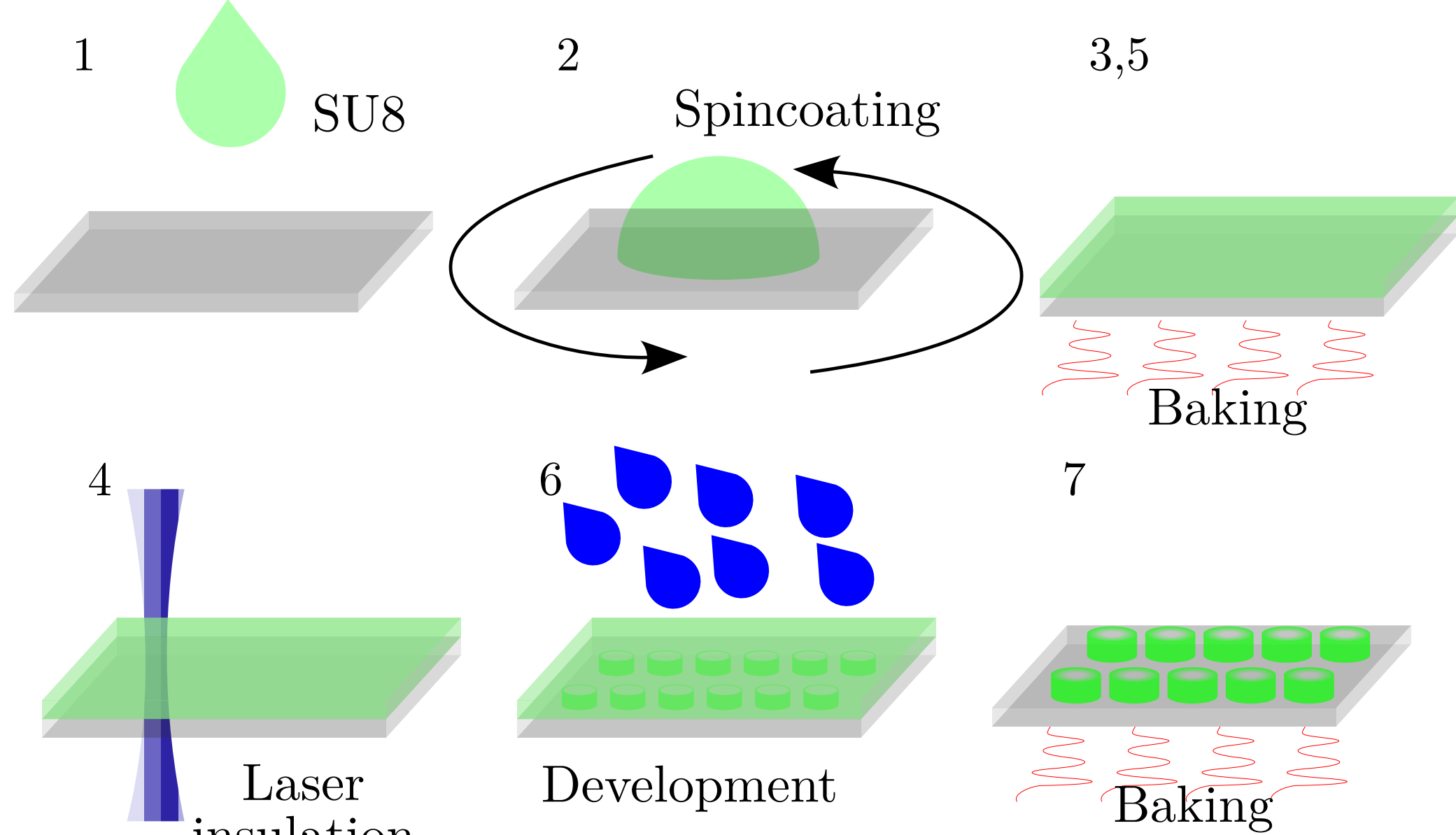
## Dispersing Quantum Dots onto the Microdisks : the Infusion Method



### Infusion Process of Microdisks

- 1 : A drop of exchanged QDs dispersed in cyclopentanone is poured onto a coverslip covered with microdisks
- 2 : Infusion is left ongoing for 5 minutes
- 3 : After several rinsing steps, we obtain a coverslip with microdisks covered with quantum dots

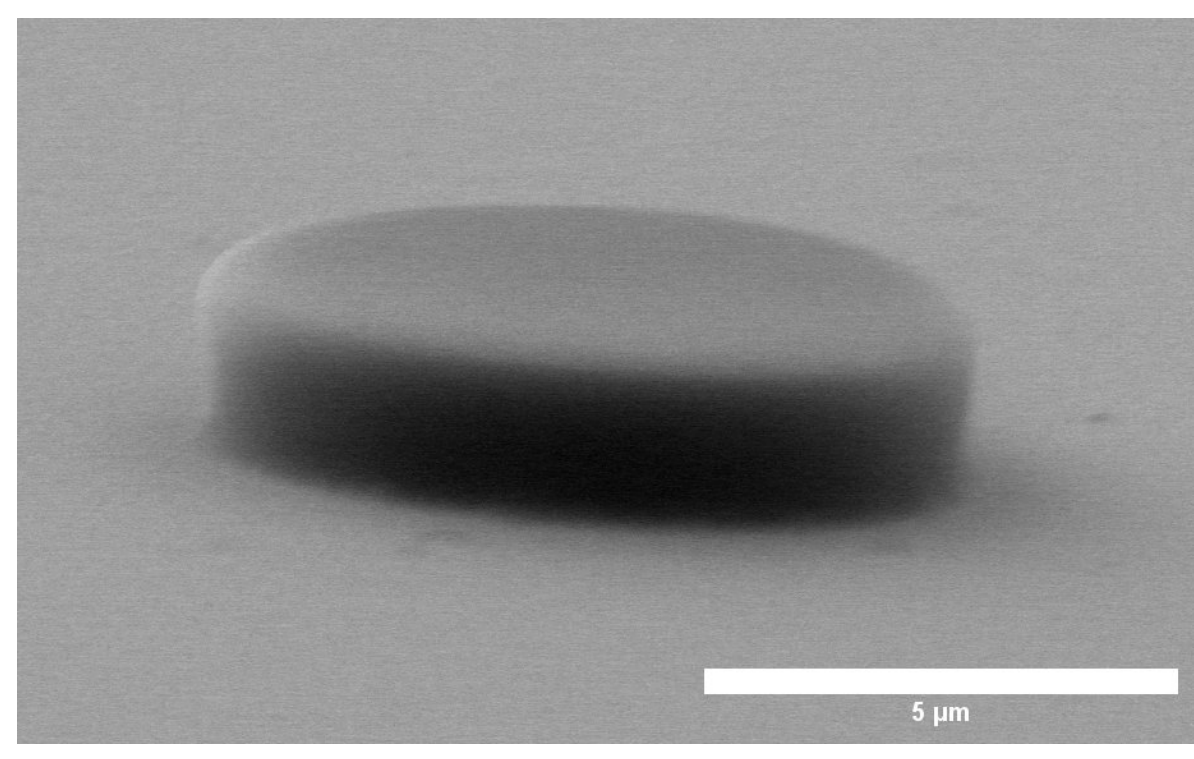
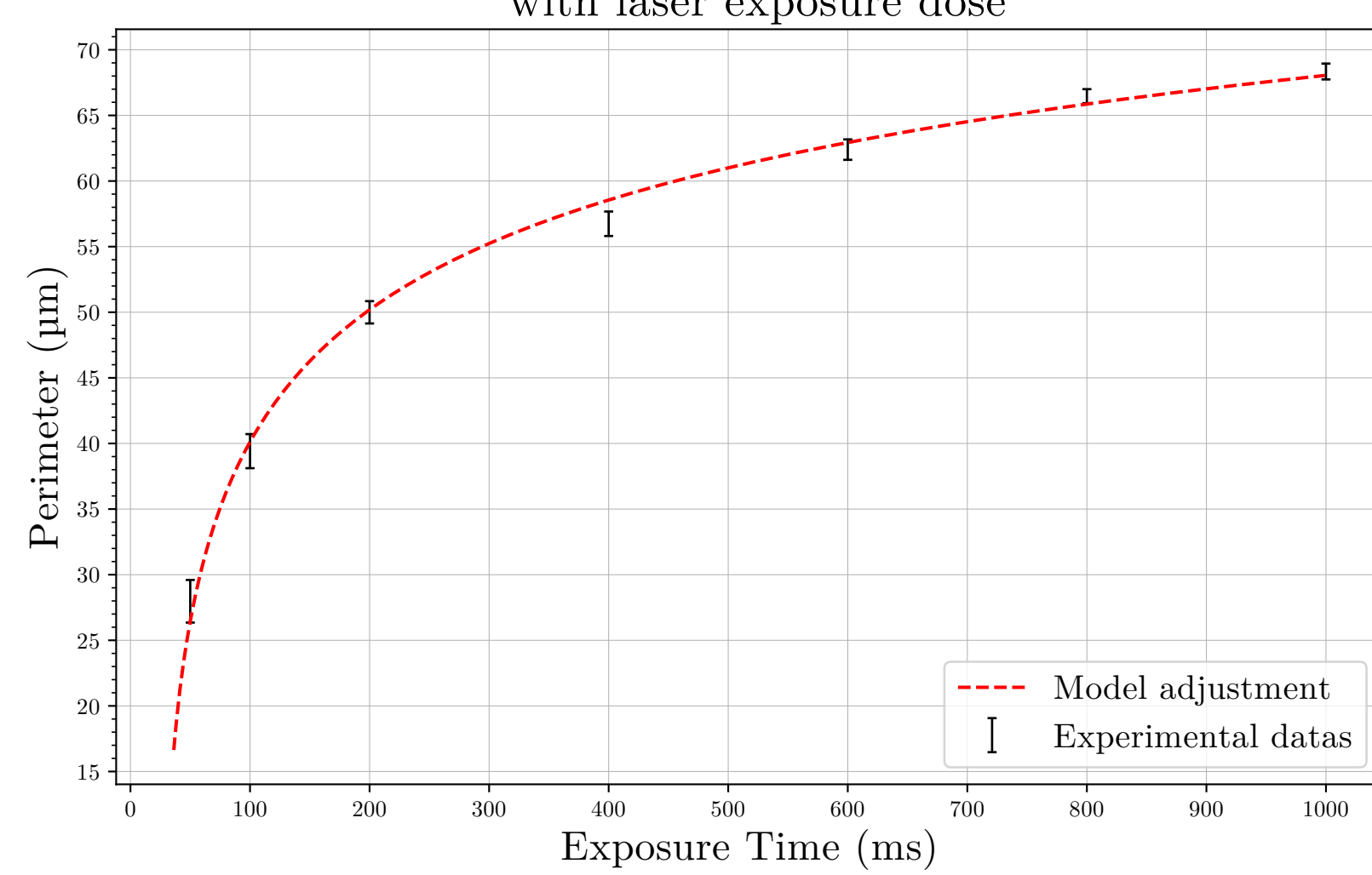
## Fabricating microdisks as Whispering Gallery Modes Microcavities using SU8



### Fabrication Process of Microdisks

- 1 : Liquid SU8 is dropped onto a gold covered glass coverslip
- 2 : Spincoating at 3000 rpm to obtain a 3µm thickness
- 3 : Soft Bake at 75°C
- 4 : Laser insolation at 405nm
- 5 : Post Exposure Bake at 95°C
- 6 : Development in PGMEA
- 7 : Hard Bake at 110°C

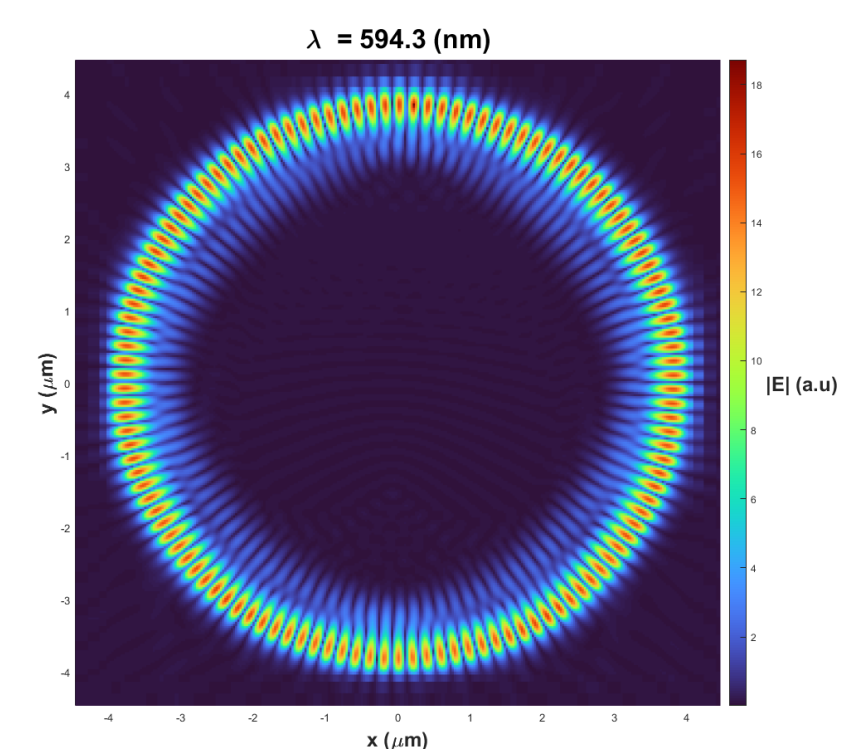
Control of microcavities diameter with laser exposure dose



SEM Image of a Microdisk

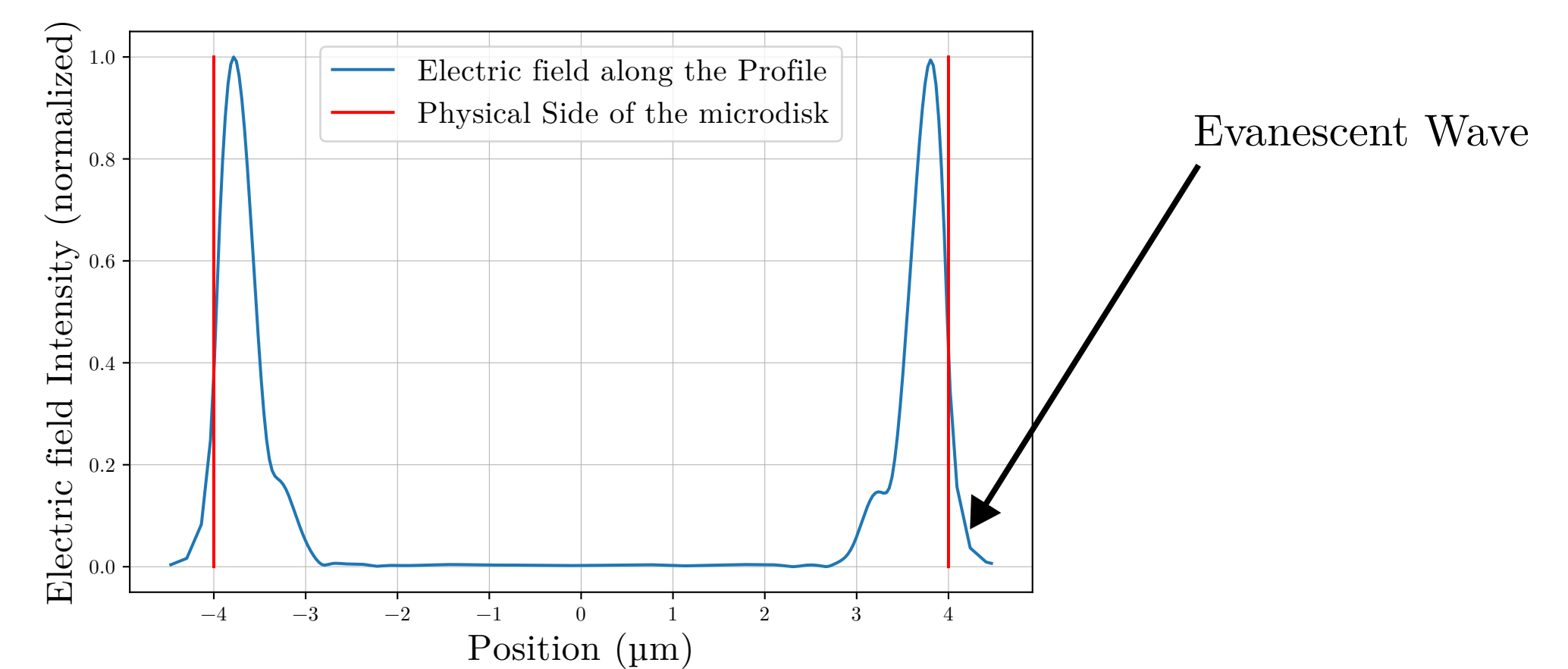
## Simulating Microdisks using FDTD

### Electric field map of a simulated Microdisk



Simulations are made using Lumerical, a software based on FDTD (Finite Difference Time Domain) calculations to get the electric field locally. Here the image shows the spatial distribution of the real part of the electric field for a given wavelength in a microdisk.

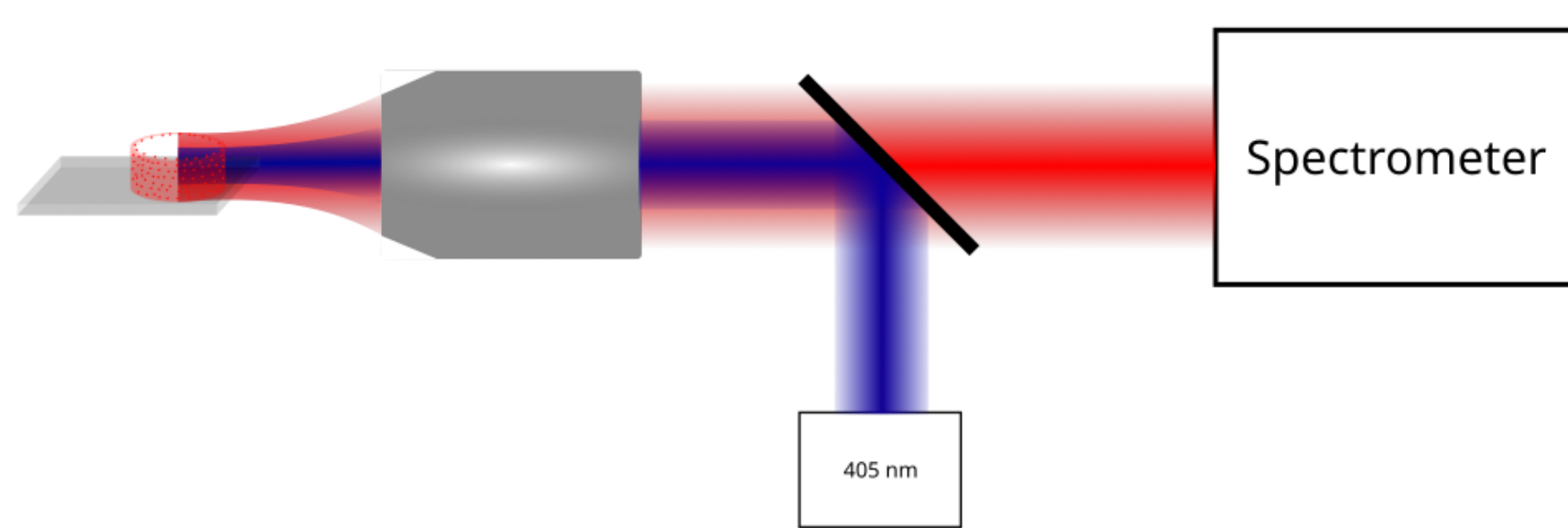
### Line Profile along the Electric Field Map



The simulated electric field spreads outside the microdisk on a few hundreds nanometers. This represents the evanescent wave which we want to use for biological detection.

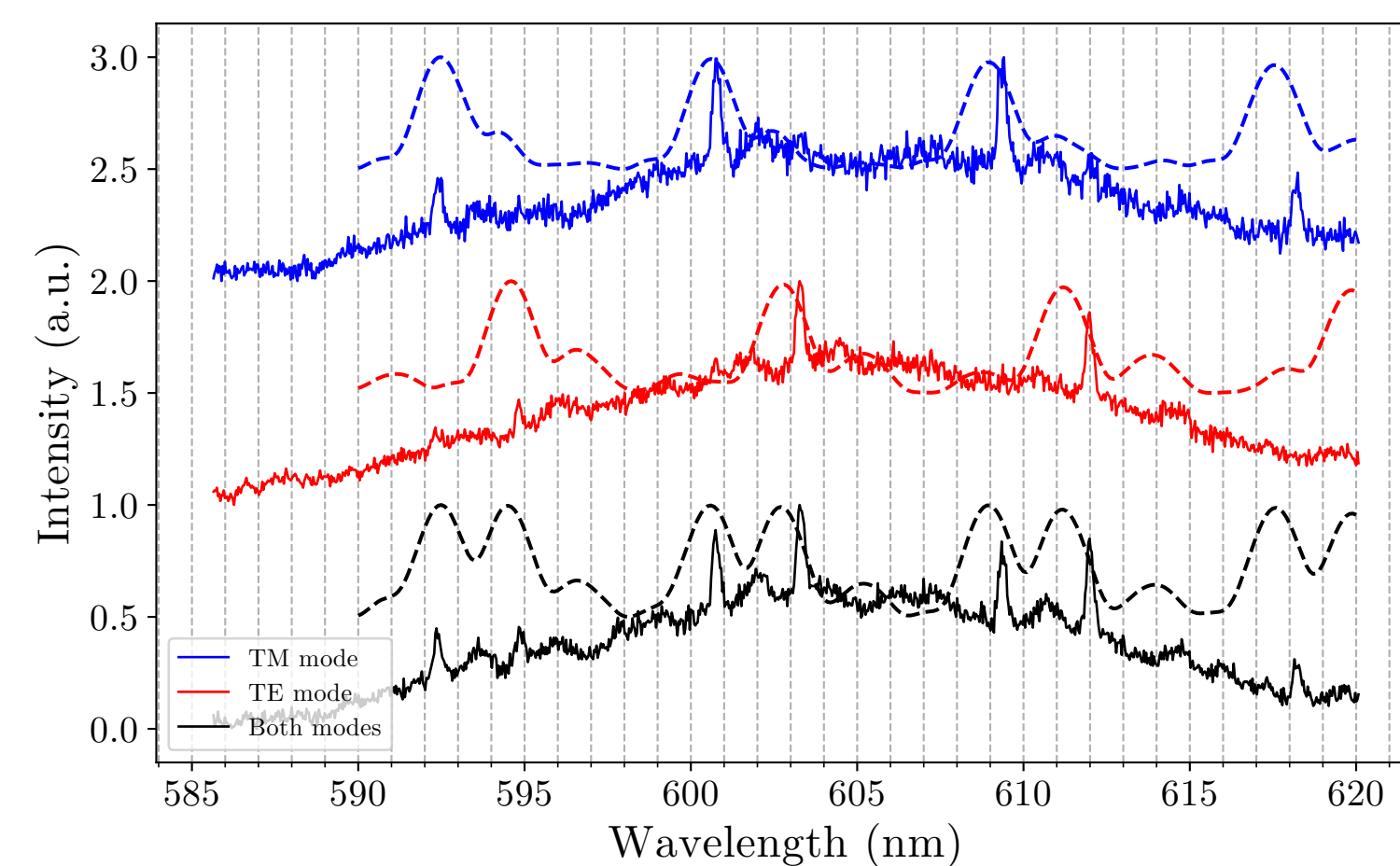
## Observation of the Whispering Gallery Modes Spectra

### Experimental Setup



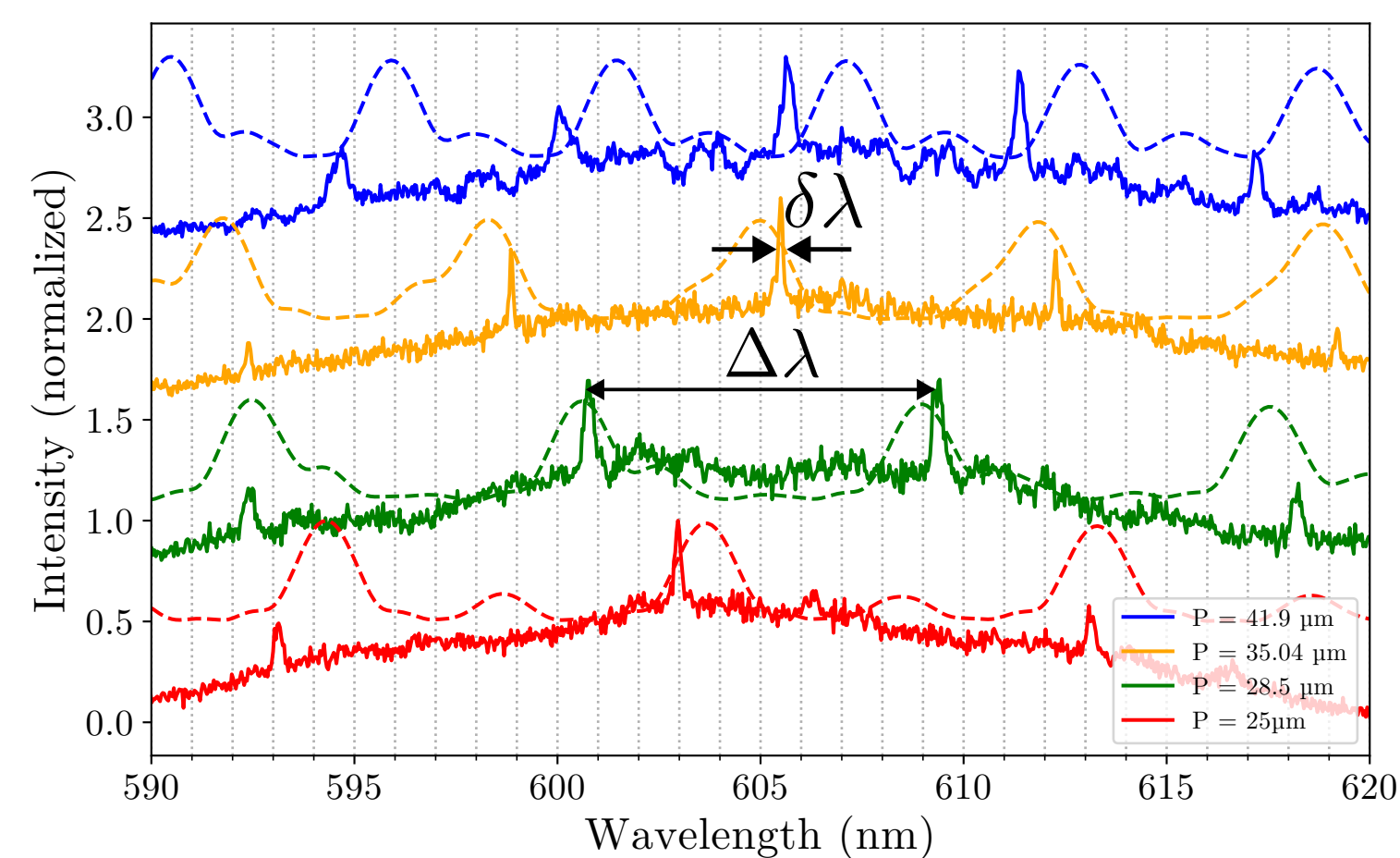
Excitation and collection are realized sideways to collect the leaks of the WGM. A polarizer was used after the dichroic to distinguish TE and TM modes. A confocal detection is used but not represented.

### Polarized detection enables discrimination between TE and TM WGMs



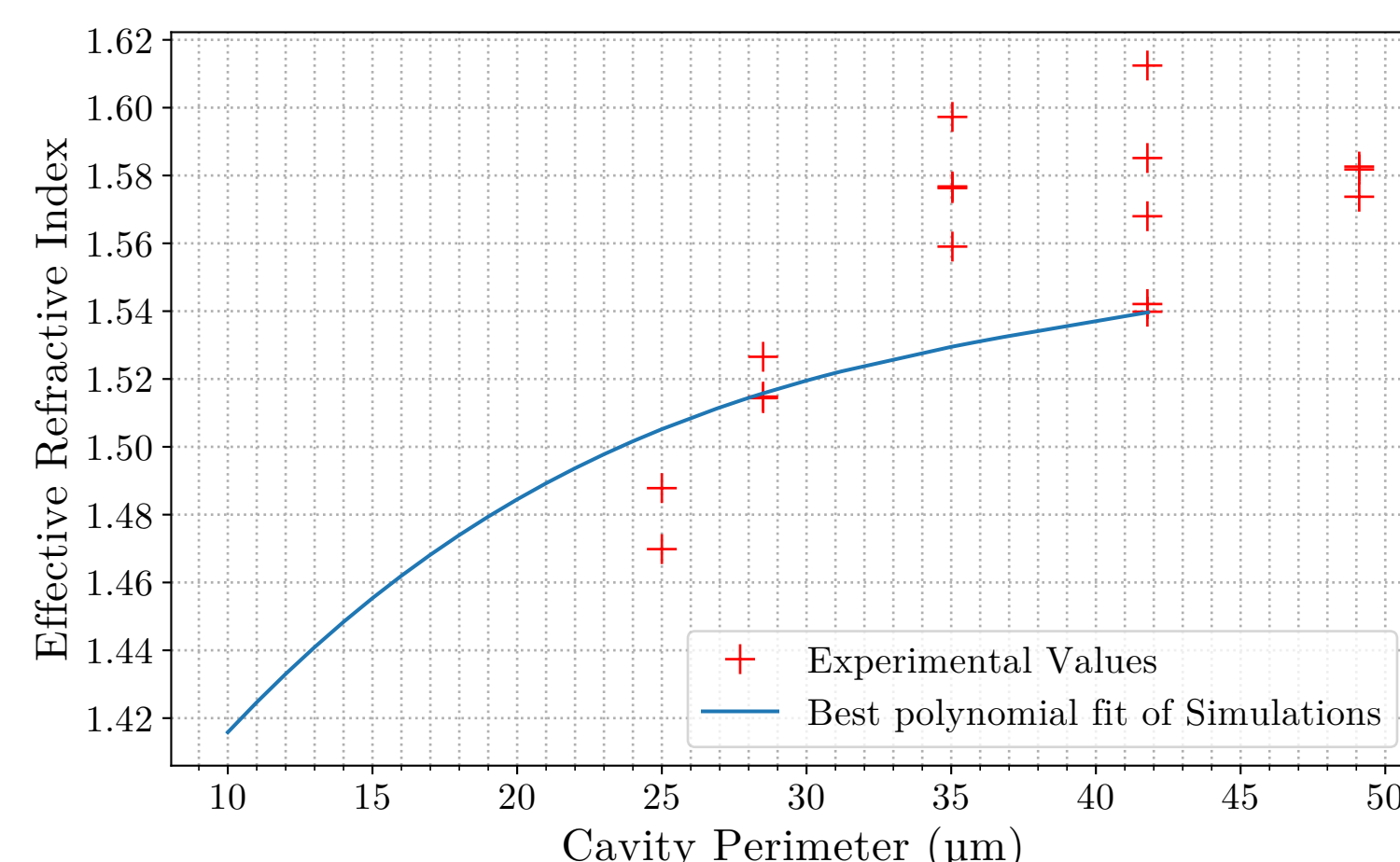
TE and TM modes see slightly different effective refractive indexes, which shifts the position of the modes. From the spectral separation between two polarization modes, we deduce a difference of effective refractive index of 0.006 between TE and TM modes.

### Effect of the microdisk diameter on the free spectral range



The continuous lines represent the experimental spectra while the dashed lines represent the simulations. The Free Spectral Range increases as the perimeter diminishes in accordance with our FDTD Simulations. Q factors as high as 6000 were measured, where we were limited by the resolution of our detection.

### The effect of the size on the effective refractive index



The difference of effective refractive index according to the microdisks size is not due to an actual change of refractive index of the microdisks, but to the spatial extension of the modes that extend more outside of the microdisks when they get smaller, leading to a diminution of the effective refractive index.

### The useful equations

$$\Delta\lambda = \frac{\lambda^2}{Perimeter * n_{eff}} \quad Q = \frac{\lambda}{\delta\lambda}$$

Q : quality factor  
n<sub>eff</sub> : effective refractive index

## Conclusions

- optimization of the fabrication of microdisk by photolithography
- homogeneous incorporation of QDs into the microdisks obtained thanks to surface modification of QDs
- observation of high quality (Q > 6000) WGMs
- FDTD modeling of the effect of polarization and microdisk perimeter on WGM properties

## Perspectives

- Lasing operation of QD-labeled microdisks
- Bio-functionalization towards biosensing
- Shape modifications of the microdisks to improve mode confinement

